

THREE NEW BIS(ACYLHYDRAZONE) MONONUCLEAR TRANSITION METAL COMPLEXES: SYNTHESIS, CHARACTERIZATIONS AND DNA INTERACTION STUDIES

Sultan KINCAL*, Faculty of Science, Department of Chemistry, Mugla Sıtkı Koçman University, Mugla, Turkey, sultankincal@mu.edu.tr

([id](https://orcid.org/0000-0003-3865-9671)) <https://orcid.org/0000-0003-3865-9671>)

Tolga GÖKTÜRK, Faculty of Science, Department of Chemistry, Mugla Sıtkı Koçman University, Mugla, Turkey, tolgagokturk@mu.edu.tr

([id](https://orcid.org/0000-0002-7234-8079)) <https://orcid.org/0000-0002-7234-8079>)

Cansu TOPKAYA, Faculty of Science, Department of Chemistry, Mugla Sıtkı Koçman University, Mugla, Turkey, cansutopkaya@mu.edu.tr

([id](https://orcid.org/0000-0002-6834-4841)) <https://orcid.org/0000-0002-6834-4841>)

Ramazan GÜP, Faculty of Science, Department of Chemistry, Mugla Sıtkı Koçman University, Mugla, Turkey, rgup@mu.edu.tr

([id](https://orcid.org/0000-0001-5731-6733)) <https://orcid.org/0000-0001-5731-6733>)

Received: 28.04.2023, Accepted: 07.08.2023

*Corresponding author

Research Article

DOI: 10.22531/muglajsci.1289197

Abstract

In recent years, studies on the design and synthesis of artificial nucleases with biological, structural and coordination properties have been increasing. With this study, mononuclear complex compounds were obtained with Cu(II), Ni(II) and Zn(II) transition metal ion salts of bis(acylhydrazone) ligand, which has the potential to show biological activity and has revolving atoms such as N and O in its structure. The characteristic structures of the obtained complex compounds were elucidated using various techniques such as FTIR, UV-Visible, ¹H-NMR, TGA, elemental analysis and magnetic susceptibility. The DNA-binding activities of potential artificial metallonucleases, whose structures were elucidated, were investigated using the UV-visible absorption titration method. Additionally, their DNA-cleavage activities were analyzed using the agarose gel electrophoresis method. The DNA binding mode and cleavage mechanisms were determined as part of this study. In line with the results obtained, it was determined that the binding mode between DNA and the complexes is a noncovalent interaction. It has been demonstrated that the compounds cleavage DNA both oxidatively and hydrolytically. It has been revealed that the radicals involved in DNA cleavage activity are H₂O₂, superoxide and hydroxyl radicals. It was revealed that the compound with the highest cleavage and bonding interaction was the Cu(II) complex, followed by Ni(II) and Zn(II) complexes.

Keywords: bis(acylhydrazones), metal complexes, DNA interactions

ÜÇ YENİ BİS(AÇILHİDRAZON) MONONÜKLEER GEÇİŞ METALİ KOMPLEKSİ: SENTEZ, KARAKTERİZASYON VE DNA ETKİLEŞİM ÇALIŞMALARI

Özet

Son yıllarda biyolojik açıdan aktif ve yapısında metal içeren yapay nükleazların tasarlanması ve sentezine yönelik çalışmalara giderek çoğalmaktadır. Gerçekleştirilen bu çalışma ile biyolojik aktivite gösterme potansiyeli olan ve yapısında N ve O gibi donör atomlar bulunduran bis(açilhidrazon)ligandın Cu(II), Ni(II) ve Zn(II) geçiş metal iyon tuzlarıyla mononükleer kompleks bileşikler elde edilmiştir. Elde edilen kompleks bileşiklerin karakteristik yapıları, FTIR, UV-Görünür, ¹H-NMR, TGA, elemental analiz ve magnetic süssebilite gibi çeşitli teknikler kullanılarak aydınlatılmıştır. Yapıları aydınlatılan potansiyel yapay metallonükleazların UV-vis. adsorbsiyon titrasyon metodu ile DNA-bağlanma, agaroz jel elektroforez yöntemi ile de DNA-kesme aktiviteleri incelenmiştir. DNA bağlanma modu ve kesme mekanizmaları belirlenmiştir. Elde edilen sonuçlar doğrultusunda, DNA ile kompleksler arasındaki bağlanma modunun nonkovalent bir etkileşim olduğu belirlenmiştir. Bileşiklerin hem oksidatif hem de hidrolitik olarak DNA'yı kestiği ortaya konulmuştur. DNA kesme aktivitesinde rol alan radikallerin H₂O₂, superoksit ve hidroksil radikalleri olduğu ortaya çıkarılmıştır. Kesme ve bağlanma etkileşiminin en yüksek olduğu bileşiğin Cu(II) kompleksi olduğu ve bu sıralamayı Ni(II) ve Zn(II) komplekslerinin izlediği ortaya konmuştur.

Anahtar Kelimeler: bis(açilhidrazon)lar, metal kompleksler, DNA etkileşim

Cite

Kincal, S., Göktürk, T., Topkaya, C., Güp, R., (2023). "Three New Bis(Acylhydrazone) Mononuclear Transition Metal Complexes: Synthesis, Characterizations and DNA Interaction Studies", Mugla Journal of Science and Technology, 9(2), 36-45.

1. Introduction

Acylhydrazones are a class of Schiff base compounds that are formed through the reaction of aldehydes or ketones with acylhydrazides. Due to the presence of active oxygen and nitrogen atoms in their structures, they are capable of forming coordination compounds with various geometries. These complex compounds, when formed with different transition metal ions, exhibit notable biological activities [1-10].

Bisacylhydrazone ligands and their complexes, designed with highly active bioelements such as Cu, Ni, and Zn, hold significant importance in the field of bioinorganic chemistry. These compounds are known for their remarkable antitumor, antibacterial, antimicrobial, and antioxidant properties [3, 11-16].

In this study, a new 5-dentate ligand, (N',N''E,N',N''E)-N',N''-(1,1'-(pyridine)-2,6-diyl)bis(ethane-1-yl-1-ylidene)) bis(4-hydroxybenzohydrazine), was synthesized by reacting 4-Hydroxybenzoylhydrazine with 2,6-diacetylpyridine. Cu, Ni, and Zn complexes of the ligand were also synthesized. The structures of the compounds were characterized using IR, ¹H-NMR, TGA, elemental analysis, magnetic susceptibility, and UV-vis spectroscopic methods.

Furthermore, the comparative DNA binding and cleavage activities of the new bis acyl ligands and their complexes were investigated.

2. Experimental

2.1. Materials and Measurements

Chemicals were obtained from Merck and Sigma-Aldrich and all substances are of analytical purity. pBR322 DNA was purchased from Fermentas.

IR spectra were taken with a 4000 to 400 cm⁻¹, Thermo-Scientific, Nicolet iS10-ATR model spectrophotometer. ¹H-NMR analyzes of synthesized compounds were taken with a Mercury-300BB model device. The melting points of the synthesized compounds were determined with the Büchi SMP-20 model device and elemental analyzes were made with LECO, CHNS-932 instrument. Thermogravimetric degradation analyzes of synthesized compounds were performed with PerkinElmer TGA 4000 model device. magnetic moment measurements were determined with Sherwood Scientific MK1 model device. UV spectra were taken with a PG brand UV-T80+ model UV-Vis spectrophotometer. The XRD analyzes of the powder samples were recorded with a Rigaku Corporation X-ray diffractometer (Model smartlab) analyzer in the Central Laboratory at Mugla Sıtkı Koçman University.

2.2. Synthesis and Characterization

4-Hydroxybenzoylhydrazine was synthesized according to the literature (Figure 1)[17].

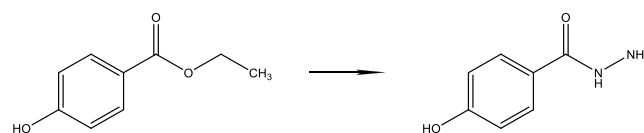


Figure 1. Synthesis of 4-Hydroxybenzoylhydrazine

4-Hydroxybenzoylhydrazine: White solid, yield: 80%, M. P.: 264-266 °C. FTIR (ATR, cm⁻¹): 3310 ν(-OH), 3193 ν(NH₂), 1622 ν(C=O), 1252 ν(C-O). Analysis (% calculated/found) for C₇H₈N₂O₂, C: 55.26/55.36, H: 5.30/5.41, N: 18.41/18.22. UV-vis (MeOH) λ_{max}: 254; 205 nm

2.2.1. Synthesis of the Ligand:

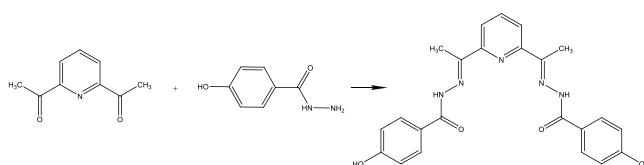


Figure 2. Synthesis of ligand

This compound was synthesized according to the literature (Figure 2) [18].

(N',N''E,N',N''E)-N',N''-(1,1'-(pyridine-2,6-diyl)bis(ethan-1-yl-1-ylidene)) bis(4-hydroxybenzohydrazine) :White solid, yield: 87%, M. P.: 247-250 °C. FTIR (ATR, cm⁻¹): 3131 ν(-OH), 2971 ν(C-H)_{Alifa}, 1666 ν(C=O), 1607 ν(C=N), 1263, 1238 ν(C-O). ¹H NMR (400 MHz, DMSO-d₆, ppm) δ 10.66 (s, 2H, -NH), δ 10.16 (s, 2H, -OH), δ 8.10 (m, 3H, Ar-H), δ 7.81, 7.75 (d, d, 4H, 4H, Ar-H), δ 2.52 (s, 6H, -CH₃). Analysis (% calculated/found) for C₂₃H₂₁N₅O₄, C: 64.03/64.05, H: 6.91/6.94, N: 16.23/16.26. UV-vis (DMF) λ_{max}: 320; 271,5 nm

2.2.2. Synthesis of Complexes [M(Lx)] (M: Cu(II), Ni(II), Zn(II)):

A suspension of 0.01 mol of ligand (ethanol) was prepared, and a solution of 0.01 mol M(AcO)₂ salt in methanol was added dropwise to the suspension. The resulting mixture was stirred under reflux for approximately 1 hour. Afterward, the mixture was cooled and filtered. The obtained solid was washed with alcohol and water, and then dried. The complexes were further purified through crystallization in a DMF-ether system.

[Cu(L)].1,5H₂O :Yield: 80%, m.p.: 320°C. B.M.: 1.71 Analysis (% calculated/found) for C₂₃H₂₂CuN₅O_{5,5} C: 53.13/54.05, H: 4.26/4.68, N: 13.47/13.75, Cu: 12.22/12.50. FTIR (ATR, cm⁻¹): 3168 ν(OH) 1591 ν(C=N-N=C), 1273;1234 (C-O). UV-vis (DMF) λ_{max}:410,5; 340,0; 270,0

[Ni(L)].2H₂O Yield: 81%, m.p.: 277 °C. B.M.: Dia Analysis (% calculated/found) for C₂₃H₂₃N₅NiO₆ C: 52.70/52.11, H: 4.42/4.57, N: 13.36/13.04, Ni: 11.09/11.25. FTIR (ATR, cm⁻¹): 3076 ν(OH) 1591 ν(C=N-N=C), 1273;1243 (C-O). UV-vis (DMF) λ_{max}: 400,0; 308,5; 282,0

[Zn(L)].1.5H₂O Yield: 86%, m.p.: 390 °C. Analysis (% calculated/found) for C₂₃H₂₂N₅O_{5.5}Zn C: 52.94/52.25, H: 4.25/4.63, N: 13.42/13.92, Zn: 12.72/12.80. FTIR (ATR, cm⁻¹): 3130 ν(OH) 1590 ν(C=N-N=C), 1272;1238 (C-O). ¹H NMR (400 MHz, DMSO-d₆, ppm) δ 9.86 (s, 2H, -OH), δ 7.91 (t, Ar-H), δ 7.76 (d, Ar-H), δ 7.62 (d, 7H, Ar-H), δ 6.73 (d, 4H, Ar-H) δ 2.41 (s, 6H, -N/C(CH₃)₃). UV-vis (DMF) λ_{max}: 412,5; 338,0; 271,5.

2.3. Biological Studies

The procedure and details of DNA binding and DNA cleavage activity studies are given in the supplementary information section.

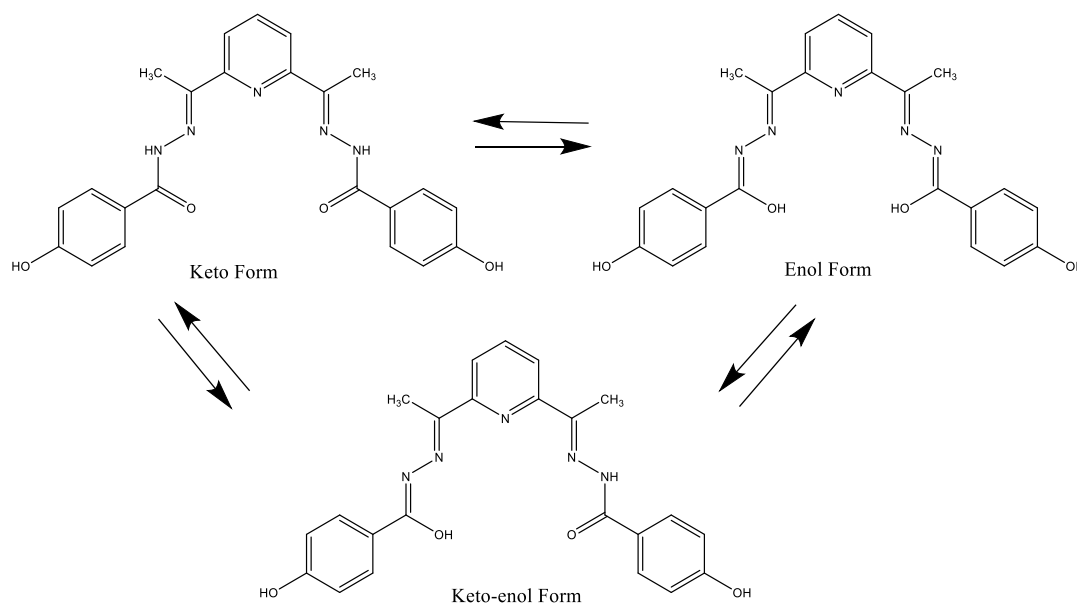


Figure 3. Tautomeric forms of the ligand

3. Results and discussion

3.1. IR Spectra

In the IR spectrum of the ligand containing bis(acylhydrazone), stretching vibration peaks of the hydroxyl group appeared at 3131 cm⁻¹. The peaks corresponding to the stretching vibrations of the amide I and azomethine groups in the ligand were observed at 1666 cm⁻¹ and 1607 cm⁻¹, respectively. Additionally, a characteristic peak corresponding to the C=N stretching in the pyridine ring was observed at 1504 cm⁻¹ [15,19] (Figure S)

In order to determine the coordination modes of the compounds, the IR spectra of the free ligand and the IR spectra of the metal complexes were compared (Fig S7-S9). In all the IR spectra of bis(acylhydrazone) complexes containing 2,6-Diacetylpyridine, broad peaks corresponding to the -OH group were observed around 3100 cm⁻¹. This observation suggests that the hydroxyl group in the para-position is not involved in coordination with the metals.

In the IR spectra of all complexes, after deprotonation of the enol tautomeric form of the ligand, the -NH band disappears as a result of the coordination of the enolic oxygen to the copper(II) ion, and a new generation occurs at 1603 cm⁻¹, probably due to the conversion of the amide (C=N) peak to the C=N-N=C stretching vibration band is observed (Figure 3).

It has been predicted that the new bis(acylhydrazone) enters coordination from enolic oxygen, azomethine nitrogen and pyridine ring nitrogen as a result of deprotonation. The new intense single peaks appearing around 1590-1600 cm⁻¹ are thought to be caused by the overlapping of the bands of the C=N group in the free ligand and the bands of the second C=N group, which is formed by the conversion of the ligand to the enol form during coordination. In addition, the shift of the C-N peak of the pyridine ring observed at 1504 cm⁻¹ in the free ligand to 1485 cm⁻¹ in the complexes is an indication that

Table 1. IR spectrum values of compounds

Compound	$\nu(-OH)$	$\nu(NH_2)$	$(C-H)_{Alifa}$	$\nu(C=O)$	$\nu(C=N)$	$\nu(C-O)$	$\nu(C=N-N=C)$
I	3310	3193		1622		1252	
L	3131		2971	1666	1607	1263,1238	
[Cu(L)].1.5H ₂ O	3168					1273;1234	1591
[Ni(L)].2H ₂ O	3076					1273;1243	1591
[Zn(L)].1.5H ₂ O	3130					1272;1238	1590

this group has entered into coordination [20]. The IR spectra of the complexes show that the newly synthesized acylhydrazones generally behave as dianionic and O,N,N',O' pentad ligands (Table 1.).

3.2. Magnetic Susceptibility Measurements

The magnetic susceptibility measurements performed at room temperature revealed that the zinc complex exhibited diamagnetic behavior, consistent with the expected behavior for metal ions possessing a d^{10} electronic configuration [21].

The magnetic moment analysis of the nickel(II) complex, characterized by its red color, indicated a diamagnetic nature.

The Cu(II) complex exhibits paramagnetic behavior at room temperature. The observed magnetic moment values for the mononuclear Cu(II) complex were measured to be 1.71 BM, which falls within the expected range for mononuclear copper(II) complexes (1.73 BM) containing a single Cu(II) cation with a d^9 electronic configuration [22].

The magnetic data analysis reveals that mononuclear copper(II) complexes, which possess an octahedral coordination environment facilitated by the additional axial coordination of ligand molecules, adopt a high-spin configuration.

3.3. NMR Spectra

In the 1H NMR spectrum of the bis(acylhydrazone) ligand, the hydroxyl group located at the para-position of the phenol ring exhibited a singlet signal, indicating the presence of two hydrogen atoms, resonating at approximately 10.16 ppm. Another singlet peak corresponding to the -NH protons was observed at around 10.66 ppm. In the ligand incorporating 2,6-diacetylpyridine, the methyl protons adjacent to the imine group were observed at approximately 2.52 ppm [23]. Furthermore, the protons associated with the pyridine ring displayed chemical shifts ranging from 8.10 to 7.75 ppm (Figure S10).

Upon examination of the 1H NMR spectrum of the [Zn(L)].1.5H₂O and [Ni(L)].2H₂O complexes, it is noteworthy that the signals corresponding to the phenol hydrogens at 9.86 and 10.00 ppm remain unaffected, indicating that these groups are not involved in the coordination process. Furthermore, the absence of the -NH peaks observed at 10.66 ppm in the ligand spectrum suggests that the enol form in the coordination sphere is bound to the metal [24]. Detailed information regarding the peaks attributed to the pyridine ring can be found in the experimental section [25] (Figure S11-S12, Table 3.).

3.4. Thermogravimetric Analysis

Thermogravimetric (TG) and derivative thermogravimetric (DTG) analyses were performed on the ligands and complexes, covering a temperature range from room temperature up to 700-900 °C. The objective was to establish correlations between the observed mass losses and the proposed compound structures. It was observed that compounds with the same structure exhibited similar thermal behaviors, indicating a consistency between the structural characteristics and the corresponding thermal properties.

The thermal degradation of the ligand exhibited a unimodal pattern, undergoing a single-step decomposition process within the temperature range of approximately 300-400 °C.

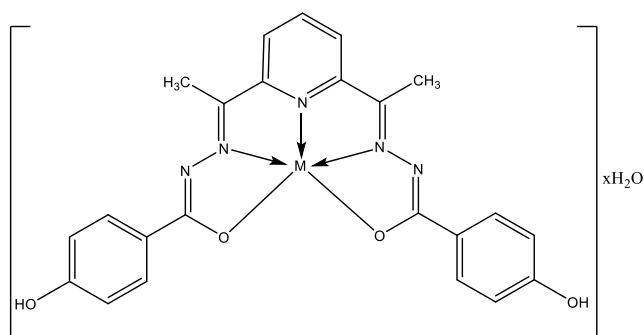
The [Cu(L)].1.5H₂O complex displayed a thermal decomposition pattern characterized by two distinct steps. The first step, below 100 °C, involved a mass loss of 4.90% (4.82%), which corresponds stoichiometrically to the removal of 1.5 moles of water molecules. Notably, this mass loss at lower temperatures suggests that the water molecule is not coordinated to the complex. The second decomposition step occurred in the temperature range of approximately 300-350 °C, leading to the formation of copper oxide [20] (Figure S1).

Table 2. ¹H NMR spectrum values of compounds

Compound	NH	OH	Ar-H	CH ₃	N/C(CH ₃) ₃
H ₂ L	10,66 (s, 2H)	10,16 (s, 2H)	8,10 (m, 3H) 7,81 (d, 4H) 7,75 (d, 4H)	2,52 (s, 6H)	-
[Zn(L)].1.5H ₂ O	-	9,86 (s, 2H)	7,91 (t) 7,66 (d) 7,62 (d)(7H) 6,73 (d, 4H)		2,41 (s, 6H)
[Ni(L)].2H ₂ O	-	10,00 (s, 2H)	7,88-7,79 (4H, t) 7,46-7,45 (4H, d) 6,87-6,84 (3H, d)	2,34 (s, 6H)	-

The thermal decomposition of [Ni(L)].2H₂O likewise occurred through a two-step process. In the first step, taking place within the temperature range of 0-100 °C, a mass loss of 6.20% (6.87%) was observed, corresponding to the removal of two moles of crystalline water. Subsequently, in the second step at temperatures between 300-400 °C, the ligand molecule underwent degradation, leading to the formation of nickel oxides [20] (Figure S2).

The thermal gravimetric decomposition of the [Zn(L)].1.5H₂O complex proceeded in two distinct steps. The first step, below 100 °C, resulted in a mass loss of 5.2% (4.81%), attributed to the removal of water molecules. It is inferred that these water molecules are not coordinated to the complex. The second degradation step, occurring above 400 °C, involved the decomposition of the ligand and the formation of zinc oxide (Figure S3).



M: Cu and Zn, x: 1.5, M: Ni, x:2

Figure 4. Estimated of structure of the complexes

3.5. XRD Analysis

Due to the inability to obtain suitable single crystals for single crystal X-ray diffraction analysis, the confirmation

of the structures of the complexes could not be achieved using this method. As an alternative, powder X-ray diffraction analysis was conducted at $2\theta = 10-70^\circ$ to obtain additional evidence regarding the structures of the metal complexes. The diffractograms obtained for the metal complexes of the newly synthesized acylhydrazones can be found in the supplementary materials.

The obtained spectra at the conclusion of this study exhibited distinct and well-defined peaks within the range of $2\theta = 5-30^\circ$, indicating the crystalline nature of all the complexes. The X-ray diffraction (XRD) patterns of the complexes displayed remarkable similarity, implying a similar structural arrangement among them. Notably, the Ni(II) complex exhibited a higher degree of crystallinity compared to the copper(II) and zinc(II) complexes, as evidenced by the line broadening observed in its crystal diffraction peak (Fig S4-S6).

3.6. UV-Vis Spectra

Upon examination of the UV-visible spectrum of 4-hydroxybenzoylhydrazine(I) in methanol, it becomes apparent that the spectrum exhibits two discernible electronic transitions. The absorption peaks observed at the shortest wavelengths, approximately at 205 nm, are attributed to $\sigma \rightarrow \sigma^*$ transitions, signifying the involvement of sigma orbitals. In addition, the broad and intense absorbances spanning the range of 254-282 nm are indicative of $n \rightarrow \pi^*$ electronic transitions, reflecting the interaction between non-bonding orbitals and pi orbitals.

The observed transitions at approximately 250 nm are attributed to the $\pi \rightarrow \pi^*$ transitions associated with the aromatic rings present in the compounds. Conversely, the third absorbance observed in the range of 300-350 nm is assigned to the $n \rightarrow \pi^*$ electronic transitions, which

arise from the interaction between non-bonding orbitals and π orbitals.

By comparing the UV-Vis spectra of the complexes with those of the ligand, a distinct blue shift in the maximum absorption bands of the ligand was observed in the complex spectra. The transitions occurring in the visible region, specifically within the range of 400-420 nm, were identified as charge transfer (CT) transitions within the complexes. Furthermore, the presence of additional peaks in the complex spectra was attributed to intra-ligand electronic transitions. These findings are consistent with the references provided [26-28] (Table 3.).

Table 3. UV-visible spectrum values of compounds

Compound	Solvent	Wavelength (nm)
I	MeOH	254; 205
H ₂ L	DMF	320; 271,5
[Cu(L)].1,5H ₂ O	DMF	410,5; 340,0; 270,0
[Ni(L)].2H ₂ O	DMF	400,0; 308,5; 282,0
[Zn(L)].1,5H ₂ O	DMF	412,5; 338,0; 271,5

3.7. DNA Binding Activities

Electronic absorption spectroscopy serves as a highly effective methodology for examining the intricate interactions between metal-based drugs and CT-DNA [29]. In this context, the absorption spectra of the complex were meticulously recorded under two distinct conditions: in the absence and presence of CT-DNA, employing increasing concentrations spanning the range of 0 to 100 μ M. Comprehensive details regarding the specific spectral variations can be found in Table 4.

Upon analysis of the binding graph for the [Cu(L)].1.5H₂O complex, it was noted that the absorbance at 338.0 nm exhibited a hypsochromic shift of 2 nm, accompanied by a concurrent decrease in intensity, indicating hypochromism. The binding event also resulted in the appearance of an isobestic point at 305.5 nm in the compound's spectrum, suggesting a singular binding mode.

When analyzing the binding spectrum of the [Ni(L)].2H₂O complex, a significant enhancement in absorption intensity was observed, coupled with a hypsochromic shift of 6 nm. Furthermore, the complex displayed two distinct isobestic points, specifically at 342.5 nm and 303.5 nm, respectively, indicating the presence of a dual binding mode. These findings collectively suggest a complex and intriguing binding behavior of the [Ni(L)].2H₂O complex.

The [Zn(L)].1.5H₂O complex exhibited a substantial hyperchromic effect of 23.87% along with a notable blueshift of 20 nm in the spectral band, indicative of its binding interaction with CT-DNA. A meticulous

examination of the graph revealed the complete disappearance of the peak in the visible region, accompanied by a shift of the peak at 338 nm to 308 nm. Additionally, an isobestic point was observed at 331 nm, further corroborating the binding interaction.

The addition of DNA resulted in significant modifications in the spectral profiles of the complexes. The observed changes in absorption intensity and wavelength shifts indicate distinct binding interactions between the Cu(II) and Ni(II) complexes with DNA. Conversely, the Zn(II) complex displayed an intensified absorption peak accompanied by a shift towards shorter wavelengths. These pronounced alterations in hypochromism and bathochromism suggest the involvement of electrostatic interactions or potential conformational changes in the DNA double helix [30]. Overall, these findings highlight the strong binding affinity of these complexes towards DNA and underscore their efficacy in DNA-binding applications (Fig S13-S15).

Table 4. CT-DNA binding results of synthesized compounds

Complex	λ_{max} (nm)		$\Delta\lambda$ (nm)	H (%)	$K_b(M^{-1})$
	Free	Bound			
[Cu(L)].1,5H ₂ O	338.0	336.0	2.0	14.69	3.0×10^6
[Ni(L)].2H ₂ O	282.0	276.0	6.0	-53.06	3.3×10^3
[Zn(L)].1,5H ₂ O	338.0	318.0	20.0	-23.87	1.0×10^4

3.8. DNA Cleavage Activities

According to the relevant literature, concentration-dependent cleavage experiments were conducted under controlled pH and incubation time conditions. The complexes were tested for their oxidative and hydrolytic cleavage activities on pBR322 plasmid DNA at concentrations of 5, 10, 25, and 50 μ M, in tris-HCl buffer at pH 7.6, with a 2-hour incubation period. Analysis of the concentration-dependent cleavage studies revealed that the cleavage activities of all complexes exhibited a direct correlation with their concentrations, both under oxidative and hydrolytic conditions. This trend is illustrated in Figures 5-7.

At lower concentrations, the Cu(II) complex, among the bis(acylhydrazone) ligand complexes, demonstrated the ability to cleave the pBR322 plasmid DNA at a single site. On the other hand, the Ni(II) and Zn(II) complexes showed a reduction in the percentage of Form I plasmid DNA on the gel, indicating potential cleavage activity. It is suggested that higher concentrations or variations in the incubation time may enhance the cleavage efficiency of the Ni(II) and Zn(II) complexes. Further investigations

are required to explore the optimal conditions for maximizing their cutting activity.

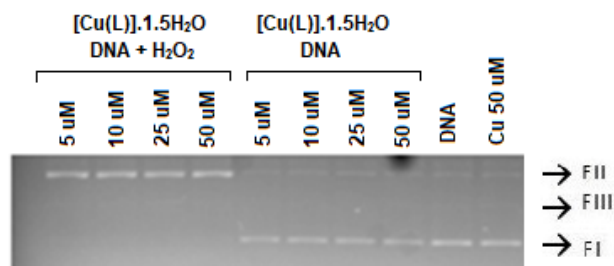


Figure 5. Concentration-dependent DNA cutting gel electrophoresis results of $[\text{Cu}(\text{L})].1.5\text{H}_2\text{O}$ complex at pH:7.6 and 2 hours incubation.

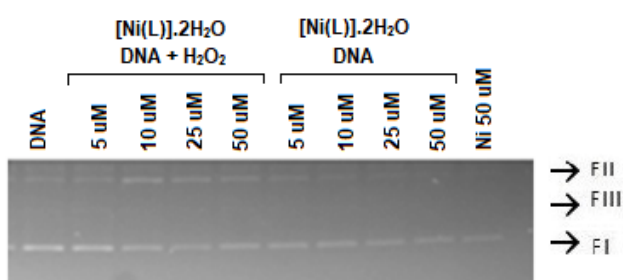


Figure 6. Concentration-dependent DNA cutting gel electrophoresis results of $[\text{Ni}(\text{L})].2\text{H}_2\text{O}$ complex at pH:7.6 and 2 hours incubation.

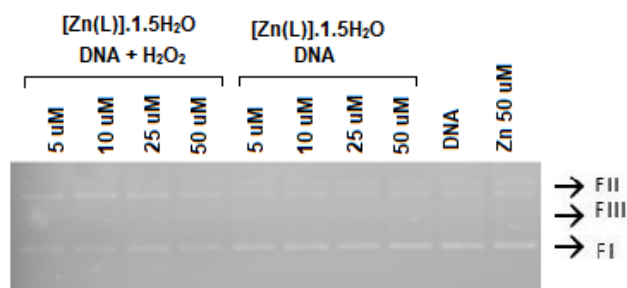


Figure 7. Concentration-dependent DNA cutting gel electrophoresis results of $[\text{Zn}(\text{L})].1.5\text{H}_2\text{O}$ complex at pH:7.6 and 2 hours incubation.

In order to obtain information about the active chemical species effecting DNA damage, the cleavage reactions were also carried out in the presence of various ROS (reactive oxygen species) scavengers, that was, catalase, superoxide dismutase, NaN_3 , DMSO and KI.

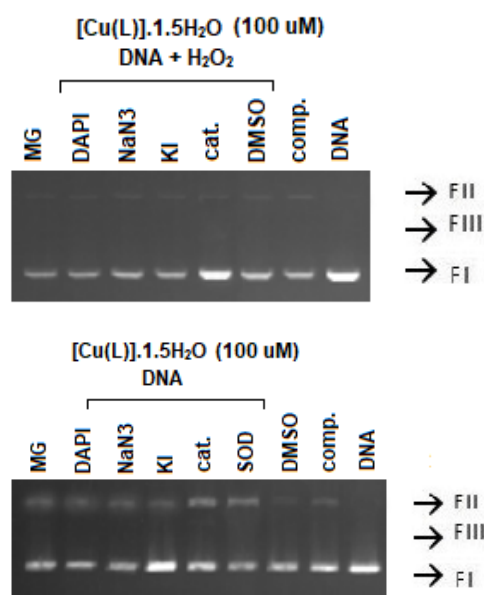


Figure 8. Oxidative (2 h) and hydrolytic (2 h) ROS mechanism study of $[\text{Cu}(\text{L})].1.5\text{H}_2\text{O}$ complex at pH:7.6 and 100 μM concentration DNA cutting gel electrophoresis results.

Upon performing competitive DNA cleavage studies with different radical scavengers in the presence of the $[\text{Cu}(\text{L})].1.5\text{H}_2\text{O}$ complex, it was observed that the oxidative cleavage activity was reduced in the presence of catalase, while the presence of other scavengers and binders did not significantly alter the activity. This suggests that the oxidative cutting activity of the complex is influenced by the presence of H_2O_2 . Similarly, under hydrolytic conditions, the decrease in activity observed in the presence of DMSO and KI indicates that the hydrolytic cleavage activity is affected by the presence of the $\text{OH}\cdot$ radical. These findings, illustrated in Figure 8, provide valuable insights into the mechanisms involved in the DNA cleavage process mediated by the $[\text{Cu}(\text{L})].1.5\text{H}_2\text{O}$ complex. In the competitive scission experiments of the $[\text{Ni}(\text{L})].2\text{H}_2\text{O}$ complex with various radical scavengers, it was found that the scission activity remained unchanged in the presence of DAPI (4,6-Diamidino-2-Phenylindole Dihydrochloride) and methyl green, both under oxidative and hydrolytic conditions. This suggests that the complex does not interact with these molecules at the binding sites. However, a significant decrease in scission activity was observed in the presence of catalase, indicating that the cutting process is influenced by the presence of H_2O_2 . These results, as shown in Figure 9, provide valuable insights into the specific role of radicals, particularly H_2O_2 , in the scission activity of the $[\text{Ni}(\text{L})].2\text{H}_2\text{O}$ complex.

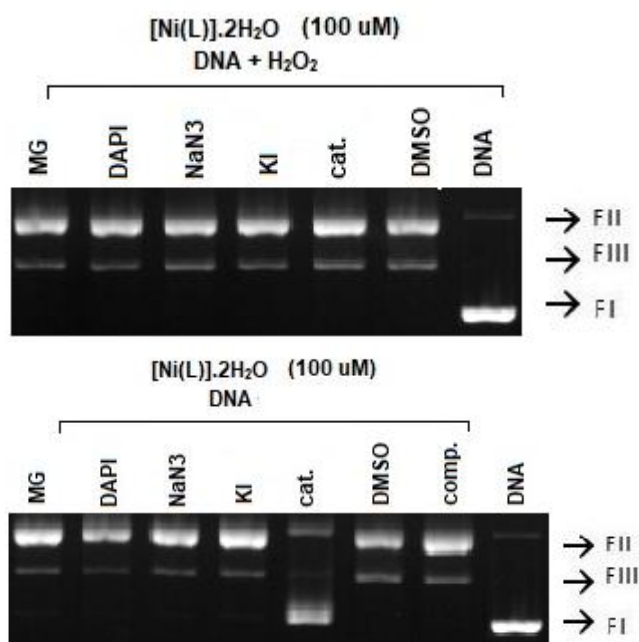


Figure 9. Oxidative (2 h) and hydrolytic (2 h) ROS mechanism study of $[\text{Ni}(\text{L})].2\text{H}_2\text{O}$ complex at pH:7.6 and 100 μM concentration DNA cutting gel electrophoresis results.

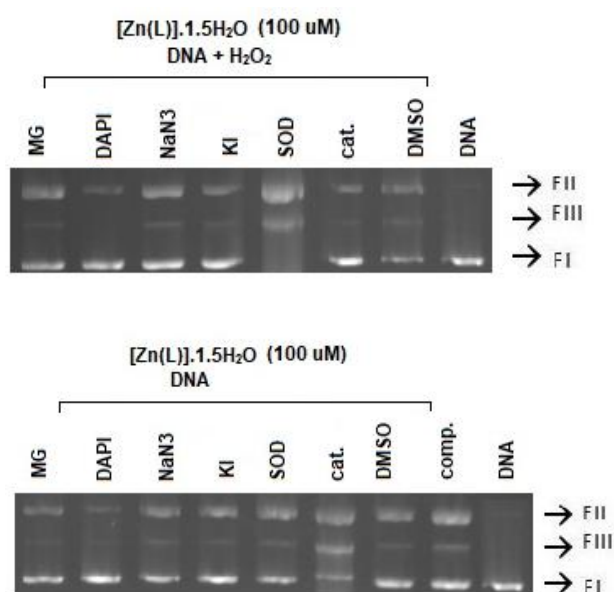


Figure 10. Oxidative (2 h) and hydrolytic (2 h) ROS mechanism study of $[\text{Zn}(\text{L})].1.5\text{H}_2\text{O}$ complex at pH:7.6 and 100 μM concentration DNA cutting gel electrophoresis results.

The investigation of cleavage mechanisms of the $[\text{Zn}(\text{L})].1.5\text{H}_2\text{O}$ complex revealed similar findings to the other complexes studied. The scission activity was found to decrease in the presence of catalase, indicating the involvement of H_2O_2 radical in the cleavage process under both hydrolytic and oxidative conditions. Furthermore, the presence of DAPI and MG (methyl green) did not result in a decrease in the cleavage activity of the complexes, suggesting that the complex does not

bind to these molecules at the active sites. These observations, as illustrated in Figure 10, provide further support for the role of H_2O_2 radical in the cleavage activity of the $[\text{Zn}(\text{L})].1.5\text{H}_2\text{O}$ complex.

4. Conclusion

In this study, three new metal complexes of Schiff base hydrazones were successfully synthesized and characterized using various spectroscopic techniques. Among these complexes, the Cu(II) complex demonstrated a higher affinity for DNA binding compared to the Ni(II) and Zn(II) complexes. The DNA cleavage experiments revealed that the cleavage activity of the complexes was concentration and time dependent, exhibiting distinct patterns in the presence of H_2O_2 . Remarkably, even at low concentrations, the copper complex displayed efficient plasmid pBR322 cleavage, targeting a single chain. Conversely, the Ni(II) and Zn(II) complexes exhibited a reduction in the Form I percentage of plasmid DNA on the gel, suggesting their cleavage activities. At higher concentrations, all complexes exhibited the ability to degrade supercoiled DNA into smaller fragments. Furthermore, in the absence of an oxidant agent, all complexes exhibited slight nuclease activity as they induced a slight conversion from form I to form II.

Based on the mechanism studies, it has been determined that the complexes with high cleavage activity are primarily influenced by molecules such as H_2O_2 , superoxide, and $\text{OH}\cdot$ radicals. These reactive species play a crucial role in demonstrating the cleavage activity of the complexes.

5. Acknowledgment

TUBITAK (Project Number: 112T315) funded this research.

6. References

- [1] Lin, Y. Q., He, S. X., Tian, X. M., Huang, C., Chen, D. M. and Zhu, B. X., "Synthesis, crystal structures and antibacterial properties of four complexes derived from mono-or diquinoline-substituted acylhydrazone ligands", *Inorganica Chimica Acta*, 541, 121080, 2022.
- [2] Zhang, Q., Jiang, F., Huang, Y., Wu, M. and Hong, M., "Coordination-driven face-directed self-assembly of a M9L6 hexahedral nanocage from octahedral Ni (II) ions and asymmetric hydrazone ligands", *Crystal Growth and Design*, 9(1), 28-31, 2009.
- [3] Ye, X. P., Zhu, T. F., Wu, W. N., Ma, T. L., Xu, J., Zhang, Z. P. and Jia, L., "Syntheses, characterizations and biological activities of two Cu (II) complexes with acylhydrazone ligand bearing pyrrole unit", *Inorganic Chemistry Communications*, 47, 60-62, 2014.
- [4] Badiger, D. S., Hunoor, R. S., Patil, B. R., Vadavi, R. S., Mangannavar, C. V., Muchchandi, I. S. and Gudasi, K. B., "Synthesis, spectroscopic properties and biological evaluation of transition metal complexes of salicylhydrazone of anthranilhydrazone: X-ray crystal structure of copper complex", *Inorganica chimica acta*, 384, 197-203, 2012.

- [5] Dash, S. P., Panda, A. K., Pasayat, S., Dinda, R., Biswas, A., Tiekink, E. R. and Sinn, E., "Oxidovanadium (v) complexes of Aroylhydrazones incorporating heterocycles: Synthesis, characterization and study of DNA binding, photo-induced DNA cleavage and cytotoxic activities", *RSC Advances*, 5(64), 51852-51867, 2015.
- [6] Chang, H. Q., Jia, L., Xu, J., Xu, Z. Q., Chen, R. H., Wu, W. N. and Wang, Y., "Syntheses, characterizations, antitumor activities and cell apoptosis induction of Cu (II), Zn (II) and Cd (II) complexes with hydrazone Schiff base derived from isonicotinohydrazide", *Inorganic Chemistry Communications*, 57, 8-10, 2015.
- [7] Santiago, P. H., Santiago, M. B., Martins, C. H. and Gatto, C. C., "Copper (II) and zinc (II) complexes with Hydrazone: Synthesis, crystal structure, Hirshfeld surface and antibacterial activity", *Inorganica Chimica Acta*, 508, 119632, 2020.
- [8] Xu, J., Zhou, T., Xu, Z. Q., Gu, X. N., Wu, W. N., Chen, H. and Chen, R. H., "Synthesis, crystal structures and antitumor activities of copper (II) complexes with a 2-acetylpyrazine isonicotinoyl hydrazone ligand", *Journal of Molecular Structure*, 1128, 448-454, 2017.
- [9] Rocha, C. S., Bomfim Filho, L. F., de Souza, A. E., Diniz, R., Denadai, A. M., Beraldo, H. and Teixeira, L. R., "Structural studies and investigation on the antifungal activity of silver (I) complexes with 5-nitrofurand-derivedhydrazones", *Polyhedron*, 170, 723-730, 2019.
- [10] Yang, Q. Y., Cao, Q. Q., Qin, Q. P., Deng, C. X., Liang, H. and Chen, Z. F., "Syntheses, Crystal Structures, and Antitumor Activities of Copper (II) and Nickel (II) Complexes with 2-((2-(Pyridin-2-yl) hydrazono) methyl) quinolin-8-ol", *International Journal of Molecular Sciences*, 19(7), 1874, 2018.
- [11] Giziroglu, E., Aygün, M., Sarikurkcu, C., Kazar, D., Orhan, N., Firinci, E. and Gokcen, C., "Synthesis, characterization and antioxidant activity of new dibasic tridentate ligands: X-ray crystal structures of DMSO adducts of 1, 3-dimethyl-5-acetyl-barbituric acid o-hydroxybenzoyl hydrazone copper (II) complex", *Inorganic Chemistry Communications*, 36, 199-205, 2013.
- [12] Parrilha, G. L., Vieira, R. P., Rebolledo, A. P., Mendes, I. C., Lima, L. M., Barreiro, E. J. and Beraldo, H., "Binuclear zinc (II) complexes with the anti-inflammatory compounds salicylaldehyde semicarbazone and salicylaldehyde-4-chlorobenzoyl hydrazone (H2LASSBio-1064)", *Polyhedron*, 30(11), 1891-1898, 2011.
- [13] Tirkey, V., Mishra, S., Dash, H. R., Das, S., Nayak, B. P., Mobin, S. M. and Chatterjee, S., "Synthesis, characterization and antibacterial studies of ferrocenyl and cymantrenyl hydrazone compounds", *Journal of Organometallic Chemistry*, 732, 122-129, 2013.
- [14] Santini, C., Pellei, M., Gandin, V., Porchia, M., Tisato, F. and Marzano, C., "Advances in copper complexes as anticancer agents", *Chemical reviews*, 114(1), 815-862, 2014.
- [15] Gökçe, C. and Gup, R., "Synthesis, characterization and DNA interaction of new copper (II) complexes of Schiff base-aroylhydrazones bearing naphthalene ring" *Journal of Photochemistry and Photobiology B: Biology*, 122, 15-23, 2013.
- [16] Tardito, S., Bassanetti, I., Bignardi, C., Elviri, L., Tegoni, M., Mucchino, C. and Marchio, L., "Copper binding agents acting as copper ionophores lead to caspase inhibition and paraptotic cell death in human cancer cells" *Journal of the American Chemical Society*, 133(16), 6235-6242, 2011.
- [17] Jamal, R. A., Ashiq, U., Arshad, M. N., Maqsooda, Z. T. and Khanb, I. U., "4-Hydroxybenzohydrazide", *Acta Crystallographica Section E*, E65, 1764, 2009.
- [18] Gup, R., Gökçe, C. and Dilek, N., "Seven-coordinated cobalt (II) complexes with 2, 6-diacetylpyridine bis (4-hydroxybenzoylhydrazone): synthesis, characterisation, DNA binding and cleavage properties", *Supramolecular Chemistry*, 27(10), 629-641, 2015.
- [19] Gökçe, C. and Gup, R., "Copper (II) complexes of acylhydrazones: synthesis, characterization and DNA interaction", *Applied Organometallic Chemistry*, 27(5), 263-268, 2013.
- [20] Chandra, S. and Sharma, A. M., "Nickel(II) and copper(II) complexes with Schiff base ligand 2,6-diacetylpyridine bis(carbohydrazone): Synthesis and IR, mass, ¹H NMR, electronic and EPR spectral studies", *Spectrochimica Acta Part A*, 72, 851-857, 2009.
- [21] Güp, R., Gökçe, C. and Dilek, N., "Synthesis, structural characterization and DNA interaction of zinc complex from 2, 6-diacetylpyridine dihydrazone and {4-[(2E)-2-(hydroxyimino) acetyl] phenoxy} acetic acid", *Journal of Photochemistry and Photobiology B: Biology*, 144, 42-50, 2015.
- [22] López, A. T., Luckie, M. R. A., Otero, D. M., Mendieta, V. S., Escudero, R. and Morales, F., "Two-Dimensional Copper Coordination Polymer Assembled with Fumarate and 5, 5'-Dimethyl-2, 2'-bipyridine: Synthesis, Crystal Structure and Magnetic Properties", *Journal of Chemical Crystallography*, 1-8, 2022.
- [23] Schleife, F., Rodenstein, A. and Kirmse, R., Kersting, B., "Seven-coordinate Mn(II) and Co(II) complexes of the pentadentate ligand 2,6-diacetyl-4-carboxymethylpyridine bis(benzoylhydrazone): Synthesis, crystal structure and magnetic properties", *Inorganica Chimica Acta*, 374, 521-527, 2011.
- [24] Gökçe, C. and Gup, R., "Synthesis and characterisation of Cu (II), Ni (II), and Zn (II) complexes of furfural derived from aroylhydrazones bearing aliphatic groups and their interactions with DNA", *Chemical Papers*, 67(10), 1293-1303, 2013.
- [25] Popov, L. D., Shcherbakov, I. N., Levchenkov, S. I., Tupolova, Y. P., Kogan, V. A. and Lukov, V. V., "Binuclear copper(II) and oxovanadium(IV) complexes with 2,6-diformyl-4-tert-butylphenol-bis-(1' phthalazinylhydrazone). Synthesis, properties and quantum chemical study", *Journal of Coordination Chemistry*, 61(3), 392-409, 2008.
- [26] Gök, Y. and Bek [acaron] roglu, Ö., "The Synthesis and Complex Formatirn of Stererisomers of some new α -Dioximes", *Synthesis and Reactivity in Inorganic and Metal-Organic Chemistry*, 11(7), 621-631, 1981.

- [27] Gup, R. and Kirkan, B., "Synthesis and spectroscopic studies of copper (II) and nickel (II) complexes containing hydrazonic ligands and heterocyclic coligand", *Spectrochimica Acta Part A: Molecular and Biomolecular Spectroscopy*, 62(4-5), 1188-1195, 2005.
- [28] Gup, R. and Kirkan, B., "Synthesis and spectroscopic studies of mixed-ligand and polymeric dinuclear transition metal complexes with bis-acylhydrazone tetradentate ligands and 1, 10-phenanthroline", *Spectrochimica Acta Part A: Molecular and Biomolecular Spectroscopy*, 64(3), 809-815, 2006.
- [29] Mohanraj, M., Ayyannan, G., Raja, G., and Jayabalakrishnan, C., "Synthesis, characterization and in vitro biological assays of copper (II) and nickel (II) complexes with furan-2-carboxylic acid hydrazide", *Applied Organometallic Chemistry*, 31(4), e3582, 2017.
- [30] Sirajuddin, M., Ali, S. and Badshah, A., "Drug-DNA interactions and their study by UV-Visible, fluorescence spectroscopies and cyclic voltametry", *Journal of Photochemistry and Photobiology B: Biology*, 124, 1-19, 2013.